Factors Influencing Glide Path Control in Carrier Landing

TULVIO S. DURAND* AND RICHARD J. WASICKO†
Systems Technology Inc., Hawthorne, Calif.

The carrier landing process involves the interaction of ship motions, the optical landing system, the pilot/aircraft combination, air wake disturbances, and the Landing Signal Officer. Mathematical models for these elements are discussed, and methods are presented for determining operational performance indices from terminal landing error dispersion data. A new concept is described for stabilizing the optical landing system against carrier deck motions, which represent one of the most significant obstacles to safe aircraft recovery. Termed "compensated-meatball stabilization," this technique considers the dynamics of the carrier landing system elements and optimizes the Fresnel lens logic scheme for increased landing performance. Simulator experiments were performed to determine the potential accident rate reduction with this stabilization method, and the major results are presented. A significant interaction exists between an aircraft design parameter, related to the lift curve slope, and the optical landing system stabilization. The fundamental factors limiting terminal landing performance are described and several basic solutions to the problem are presented.

Introduction

THE task of landing on an aircraft carrier requires precise airplane control since the tail hook must engage one of four arrestment wires spaced only 40 ft apart. With a realistic approach speed and a 3.5° glide path, under no ship motion conditions an aircraft will nominally clear the ramp by 11 ft, touch down 1 sec later, and have an impact velocity of 13 fps. Routinely operating with such landing conditions, the U. S. Navy recorded over one quarter million carrier landings of fixed-wing aircraft during Fiscal Year 1964. In the same year, there were 88 accidents and 23 fatalities associated with carrier landings. The over-all accident rate of 3.1 per 10,000 landings was the lowest experienced up to that time by the Navy, and was more than ten times better than that for FY-1950. Still, this rate greatly exceeds conventional airfield landing accident rates, even though the majority of carrier air operations are conducted during the daytime under nearly ideal conditions of a steady deck and good weather. The Navy is continuously striving to reduce the accident rate and to extend recovery operations to more severe environments, since air operations are too often suspended because of poor weather, strong winds and turbulence, and excessive ship motions.

The moving carrier deck is one of the most significant obstacles to safe aircraft recovery, and can by itself render catastrophic terminal landing conditions. When the aircraft's inertial path is precisely controlled, the ship heave motion directly alters the ramp clearance by a 1:1 ratio and changes the touchdown point by a 14:1 ratio. Likewise, ±1° of ship pitch produces a motion of ±9 ft at the ramp and a ±80-ft change in the touchdown point. The heave and pitch motions also cause large vertical deck velocities and thus drastically reduce the available impact velocity margin. One continually problematic area with regard to carrier landings is the method for stabilizing the Fresnel Lens Optical Landing System (FLOLS), the element which produces the visual glide slope reference used by the pilot for aircraft height control.

This paper, a condensation of Ref. 1, presents results of an analytical/experimental study directed toward understanding the over-all carrier landing process and developing better FLOLS stabilization against deck motions to achieve increased landing performance. The elements of a quantitative mathematical model of the landing system are discussed, and a new FLOLS stabilization concept is described. Results of a simulator investigation of the carrier approach and landing task are presented, and a significant interaction between aircraft design considerations and FLOLS stabilization is discussed.

Presented as Preprint 65-791 at the AIAA/RAeS/JSASS Aircraft Design and Technology Meeting, Los Angeles, Calif., November 15–18, 1965; submitted June 20, 1966; revision received October 3, 1966. This research was supported by the Air Programs Division of the Office of Naval Research and cosponsored by the Naval Air Systems Command under Contract Nonr-4156(00). [8.07, 8.09, 8.15, 12.11]

* Senior Staff Engineer.
† Senior Staff Engineer; now Aerospace Technologist, NASA Headquarters, Washington, D. C. Member AIAA.

Carrier Landing System Model

Although the difficult piloting tasks of heading control, bank angle control, and lateral lineup contribute to the carrier landing problem and add to the pilot's workload, the majority of accidents result from inadequate vertical path control, and in 1964 approximately 80% of all landing accidents were ramp strikes and hard landings.[2] The significant elements of a model describing the dynamic aspects of control in the vertical plane are shown in Fig. 1 and are discussed in subsequent paragraphs.

Ship Geometry and Dynamics

The motion of the carrier deck results from the ship's response to sea wave and swell wave excitations. This motion in turn affects the FLOLS-commanded glide slope and directly contributes to terminal dispersions or errors. The result of the wave input acting through the ship's dynamic characteristics is represented by power spectral densities of ship pitch, θ_s; roll, φ_s; and heave, h_s. The rms values of the illustrated deck motions, $\sigma(\theta_s) = 1°$, $\sigma(\varphi_s) = 2.2°$, and $\sigma(h_s) = 5.5$ ft, correspond to upper limits for normal aircraft launch and recovery operations. In the dominant frequency region of the motion spectra, ship pitch leads heave by 45° to 90°; the complete phase angle relationship is presented in Ref. 3. Generic equations are given in Fig. 1 which relate beam motion h_B to deck motions, aircraft responses q_a to pilot's elevator and throttle control outputs δ_e and δ_T, and finally terminal errors to aircraft and ship motions. The other ship-dependent variables which enter into the model's assessment of absolute landing performance are arresting wire locations, ship speed and heading, and wind-over-deck; these are treated subsequently.

Fresnel Lens Optical Landing System

The Fresnel Lens Optical Landing System is used to provide a glide slope reference. Some form of lens logic is required to command the lens pitch θ_L and roll φ_L servos to respec-

tively rotate and vertically translate the beam to counteract measured deck motions. Several lens logic or stabilization schemes have been used operationally in the past. Currently, the point-stabilized system is being replaced by the newer line-stabilized method. Another lens logic scheme, compensated-meatball stabilization (CMS), was evolved in earlier work[3] and is extensively described later in this paper. The following descriptions define the characteristics of each method in terms of the optically commanded, zero-error flight path along the angled deck centerline. The path is referenced to an inertial axis system which moves with the ship's inertial velocity, U_s.

Point-stabilized

The path translates with ship heave and rotates about a point 2500 ft aft of the ship. The lens pitch servo is used to cancel the motions at the 2500-ft location that otherwise would result from ship pitch and roll. The roll servo is used for static setting of the beam tilt angle to accommodate the hook-to-eye distances of different aircraft.

Line-stabilized

The path translates with ship heave. Beam motions which would be induced by ship pitch and roll are completely removed from the visually indicated path. Both pitch and roll servos are utilized to effect beam stabilization, and are additionally used to set the basic beam angle and hook-to-eye biases.

Compensated-meatball-stabilized

The path is stabilized with respect to the horizon so that there is no angular motion. The path translation is related to the vertical motion of a point on the deck, $h_{TD/2}$, by a second-order lead transfer function, or compensation filter, and a higher frequency attenuation filter. The physical location of $h_{TD/2}$ is on the landing deck centerline, halfway between the ramp and intended touchdown point. The compensation filter's damping ratio and natural frequency are individually chosen for each aircraft type so as to achieve near-synchronization of aircraft and deck vertical motions. This stabilization scheme requires measurement of the total vertical deck motion and its derivatives, i.e., velocity and acceleration. Pitch and roll FLOLS servos are required to effect stabilization and to set the basic beam angle and hook-to-eye biases.

Pilot and Aircraft

A complete and exact model of the pilot's role in a carrier landing must represent his precognitive behavior, decision-making processes, compensatory control capability, physiological and psychological limits, etc., as well as describe inter-pilot and intrapilot variability. In later portions of this paper, some of the more subtle aspects of piloting technique in carrier approach are discussed. However, it has been found, and substantiated experimentally, that a multiple-loop compensatory pilot model suffices to describe the significant control actions in the terminal portion of carrier landing.

A conventional servo form can be used to represent the pilot in compensatory tracking tasks. This makes the pilot's error-sensing and control-actuating functions equivalent to those of an autopilot. This equivalence is not generally demonstrable in the point-by-point sense, but is observable in the short-time average sense and results in an effective linear model of the combined linear and nonlinear control behavior of the pilot. The quasi-linear input/output characteristics usually account for over 90% of the pilot's total output power. The remaining 10% or so is principally due to his time variations and sampling characteristics and, to a lesser extent, his threshold

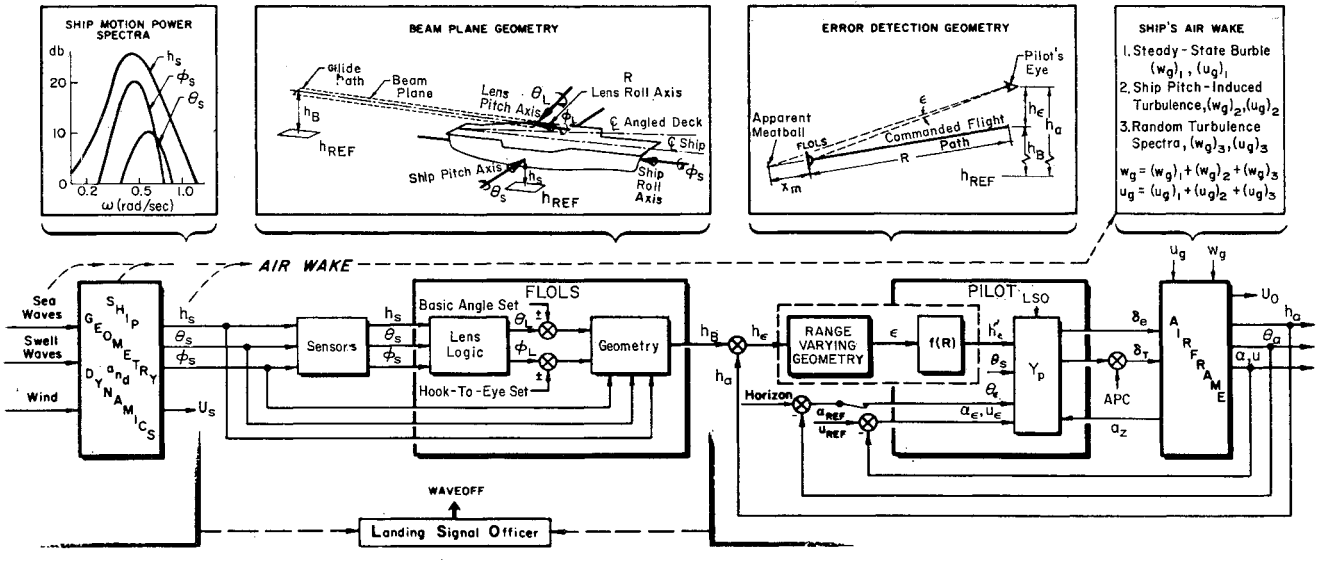

GENERIC EQUATIONS

FLOLS SERVO CONTROL LOGIC (STABILIZATION)

Pitch Servo: $\theta_L = K_1\theta_s + K_2\phi_s + K_3h_s + (\beta_0)_{set}$

Roll Servo: $\phi_L = K_4\theta_s + K_5\phi_s + K_6h_s + (h/e)_{set}$

BEAM MOTION

$$h_B = [h_s + C_1\theta_s + C_2\phi_s + C_3\phi_L] + [C_4\theta_s + C_5\phi_s + C_6\theta_L]R$$

HEIGHT ERROR GEOMETRY

FLOLS Beam Indicated	Pilot Interpreted
$\frac{\epsilon}{h_\epsilon} \doteq \frac{x_m}{R(R+x_m)}$	$\frac{h'_\epsilon}{\epsilon} \doteq \frac{R(R+x_m)}{x_m}$

AIRCRAFT MOTION

$$q_a = \frac{q_a}{u_g}u_g + \frac{q_a}{w_g}w_g + \frac{w_g}{\delta_T}\delta_T + \frac{q_a}{\delta_e}\delta_e$$

PILOT FLIGHT CONTROL

Elevator: $\delta_e \doteq K_{p_\theta}e^{-\tau s}\theta_\epsilon + K_{ph_{\delta_e}}e^{-\tau s}h'_\epsilon + [z_p(t)a_z]_{\delta_e}e^{-\tau s}a_z + \cdots$

Throttle: $\delta_T \doteq K_{ph_{\delta_T}}h'_\epsilon + K_{pu/\alpha}(u/\alpha)_\epsilon + [z_p(t)a_z]_{\delta_T}a_z + f(APC)\cdots$

TERMINAL ERRORS

Height Error Over Touchdown Point: $\Delta h_{TD} = h_a - (h_s - L_{TD}\theta_s - Y_{TD}\phi_s)$

Height Error Over Ramp: $\Delta h_R = h_a - (h_s - L_R\theta_s - Y_R\phi_s)$

Impact Velocity Error: $\Delta V_I = \dot{h}_s - L_{TD}\dot{\theta}_s + (U_0 - U_s)(\theta_s + \sin\psi_d\phi_s) - \dot{h}_a$

Fig. 1 Major elements of the landing system.

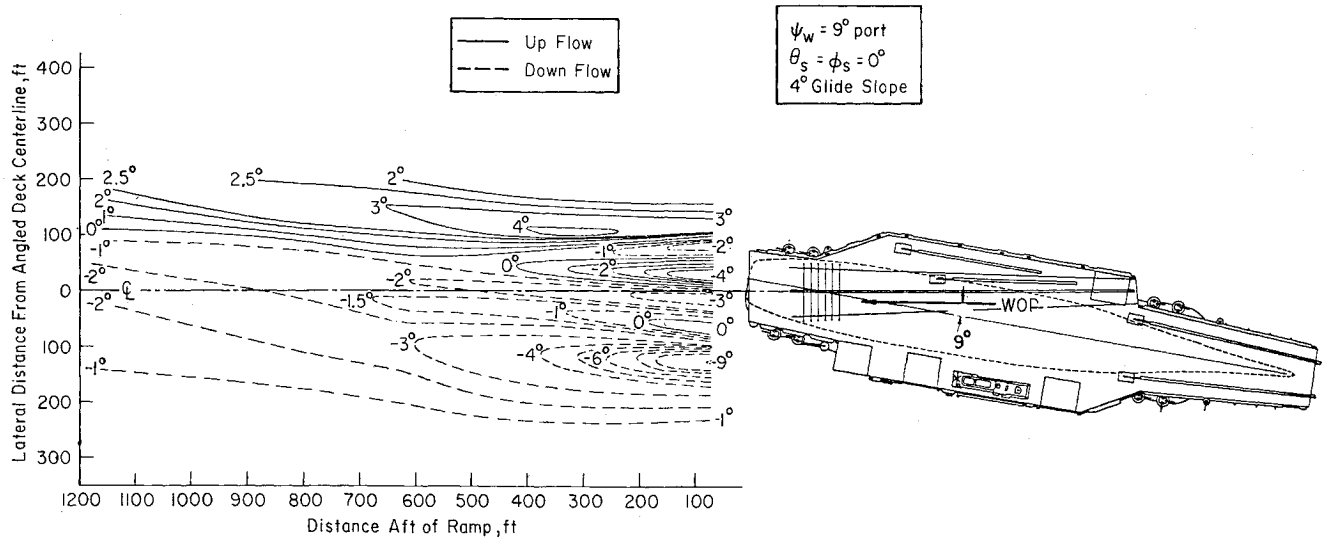

Fig. 2 Steady-state vertical flowfield astern a Forrestal class carrier.

nonlinearity. The sum total of all measured quasi-linear characteristics, when fitted by a simple general mathematical form and augmented by "rules" which explain how the form is to be adjusted (i.e., what numerical values are appropriate) for a given control situation, becomes a pilot model. Reference 4 describes some of the latest experimental and analytical work on pilot modeling activities, and Ref. 1 discusses the model used in carrier landing system analyses.

A central question is how the pilot controls his aircraft in the approach and landing in terms of visually sensed controlled motion quantities, or his inputs, and his related manipulator outputs. It has been found that the actual pilot control technique, or specific loop closures, is very dependent on the chronological approach phase, the aircraft's speed relative to the speed for minimum drag or power required, the nature and relative magnitude of the air wake, and the ship/FLOLS-beam motions. Reference 5 discusses in detail and Ref. 1 summarizes the changes in pilot control behavior with approach phase based on experimental observations of simulated approaches by carrier-qualified pilots and measured closed-loop parameters. The appropriate model for the pilot during the terminal control phase of carrier landing involves control of both pitch attitude and altitude with the elevator. For the short time of interest, 5 sec or less prior to ramp-crossing, the use of throttle to control airspeed or angle of attack is relatively unimportant, even when the aircraft is below the minimum drag speed. However, for completeness, a $u \rightarrow \delta_T$ or $\alpha \rightarrow \delta_T$ loop, similar to the flight control action of an autothrottle, is added to the pilot model in Fig. 1. Near the ramp the magnitude of height corrections is small, of the order of ± 5 ft; correspondingly, small but precise stick movements are needed. Further, elevator deflections that are used to control altitude are blended with the control actions required to maintain pitch attitude in the presence of the air wake. Therefore, when in the vicinity of the ramp the pilot may not be absolutely conscious of the exact control technique employed. Factors that must be considered in the selection of appropriate pilot gains for each of the control loops are discussed in Ref. 1.

The aircraft's longitudinal responses to pilot control inputs and turbulence during carrier approach and landing are adequately represented by simple linearized three-degree-of-freedom perturbation equations of motion. Certain airframe dimensional stability derivatives have dominant effects on the significant closed-loop pilot/aircraft system response modes; consequently, the correct simulation of a small number of basic aerodynamic effects is more important than an extensive representation of complex aerodynamic nonlinearities and cross-coupling terms in the equations of motion.

Carrier Air Wake

The air wake model has been derived from the water tunnel data of Oceanics Inc.,[6,7] and certain wind tunnel data of the David Taylor Model Basin.[8] This model consists of three separate but superposable components: steady-state flow angularity, ship-motion-induced disturbance, and random turbulence. The steady-state air wake model was derived from flow pattern plots constructed from the data of Ref. 6 and illustrated in Fig. 2. For a wind-over-deck (WOD) direction slightly starboard to the angled deck, lines of constant vertical angularity are shown in this figure for a glide path plane of 4° and depict a complicated distribution of upwash and downwash. Other WOD angles relative to the deck produce similar flowfields, but the pattern is shifted to port or starboard and approximately aligned with the WOD vector. An equivalent analysis of the horizontal component of the air wake velocity indicates a similar dependency on the WOD direction. Using a probabilistic WOD-direction model, derived from the data of Ref. 9 and explained in Ref. 1, a representative set of vertical and horizontal flow characteristics was obtained. In addition, the effects of a maximum or severe air wake on pilot control effort and resulting aircraft motions in the approach were determined. As noted in Ref. 1, although the average or probable steady-state air wake can be handled easily by tight compensatory control by the pilot, aided perhaps by a more or less constant precognitive response, the real problem with the steady-state disturbance is an encounter with extreme conditions which surprise the pilot.

Equations describing the vertical and horizontal air wake disturbances generated by carrier pitching motion are presented in Ref. 1 and represent curve-fitted amplitude and phase characteristics vs range. It is shown in Ref. 1 that this disturbance can easily excite short-period or Dutch roll oscillations, but such motions have little or no effect on the flight path, and consequently the ship-motion-induced turbulence is not of major concern. The random turbulence portion of the air wake is modeled from Ref. 7 data by first-order white noise filters, and the resulting pilot/aircraft system responses are shown in Fig. 3. These responses indicate rms height errors at the ramp as a function of pilot gains in the pitch attitude and height control loops. Reasonable height dispersions result with the gains of the pilot model used in Ref. 3. These can be further reduced by tightening up the altitude control loop, thereby permitting a greater tolerance for height errors due to the steady-state burble, i.e., errors resulting from imprecise precognitive inputs. However, such increases in altitude gain are untenable with the current

FLOLS stabilization methods because they result in steadily increasing values of the beam-motion-induced height errors.

Landing Signal Officer

In actual carrier operations, a Landing Signal Officer (LSO) monitors each pass and, on the basis of anticipated terminal conditions, decides whether to let the landing proceed or to command an abort or "waveoff." The pilot similarly judges the pass, and will in many instances initiate a voluntary waveoff. A statistical model has been formulated based on estimates by experienced pilots and LSOs of their own over-all efficiency in preventing accidents[10] and gross operational data on average waveoff rates.[11] These data and estimates suggest a bifunctional LSO model directly affecting accident and missed-landing rates according to the following effectiveness/ineffectiveness functions:

1) Waveoff of 90% of all passes which would result in an accident.
2) Waveoff of 10% of all good passes. A good pass is defined as one which would not have resulted in an accident had it been allowed to proceed. Operationally speaking, a "good" pass which, for example, clears the ramp by only a few inches, is, in fact, not an acceptable pass.

This model assumes that the LSO, in combination with the pilot, is 90% effective. In actual carrier operations, some accidents occur on passes even though a waveoff has been given. Arbitrarily, these are assigned to ineffective LSO action.

The "ninety-by-ten" average statistical model for waveoffs operates on both potential ramp strike and hard-landing accidents but does not influence the bolter rate. As will be shown later, this simple model description yields realistic landing performance estimates.

Terminal Landing Errors

The aircraft flight path is controlled to terminate with an engagement of one of the arresting wires while attaining safe margins of ramp clearance and impact velocity. The geometry representing this terminal control problem is illustrated in Fig. 4. Three probability distribution functions are illustrated, separately representing rms values of ramp height error $\sigma(\Delta h_R)$, height error at the intended touchdown point $\sigma(\Delta h_{TD})$, and impact velocity error at touchdown $\sigma(\Delta V_I)$.

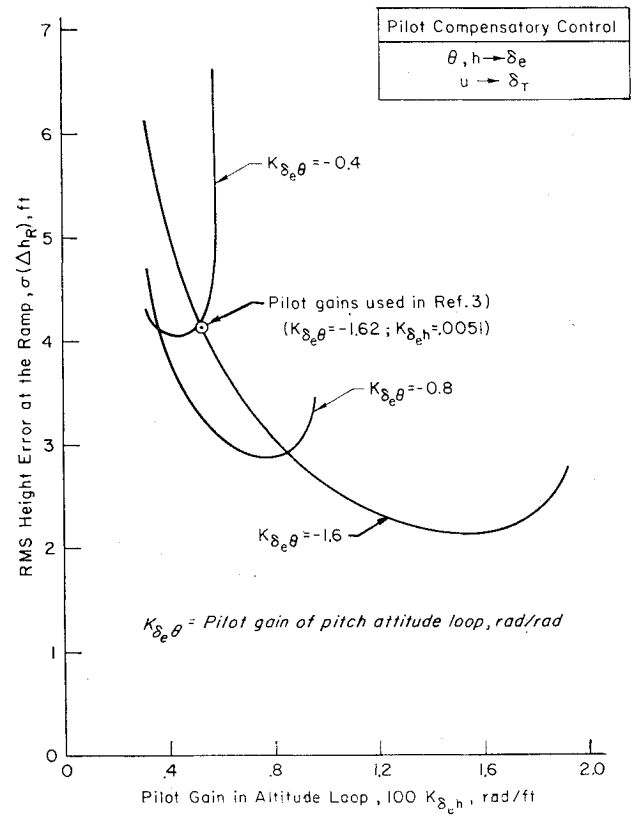

Fig. 3 Closed-loop pilot/aircraft altitude response to air wake random turbulence as a function of pilot control gains.

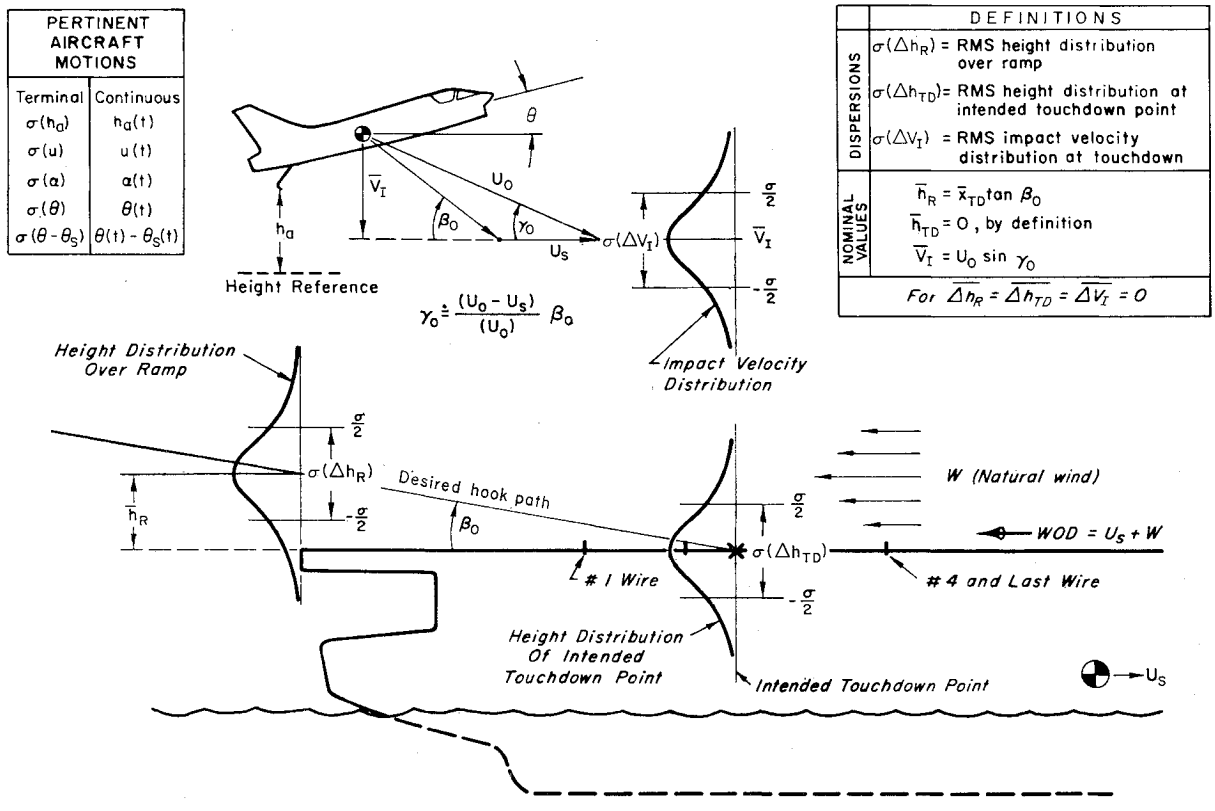

Fig. 4 Definition of landing geometry and statistical measures.

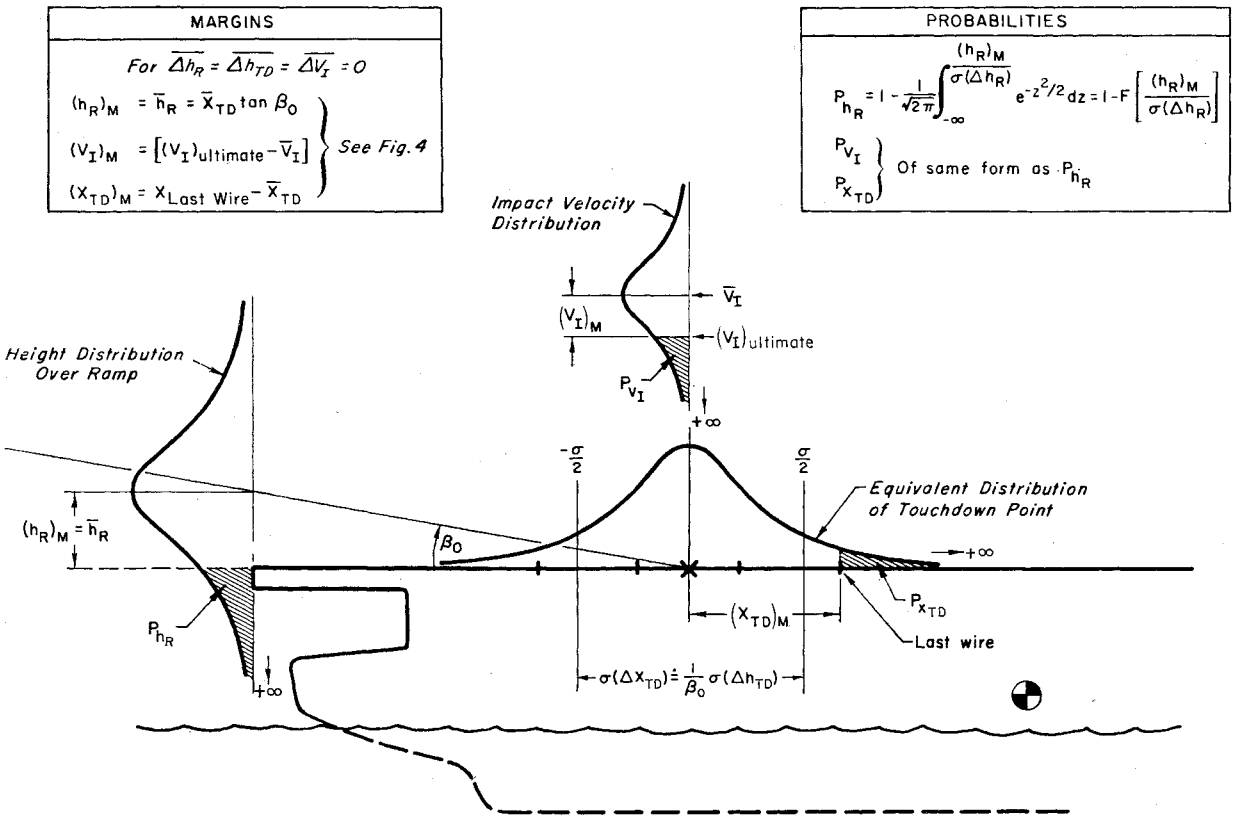

Fig. 5 Definition of margins and probabilities used in formulating the landing performance matrix.

The nominal or mean values of these distributions are set by the basic deck configuration (wire spacing and layout), the location of the FLOLS and its basic beam angle β_0, and the aircraft glide path γ_0. In turn, γ_0 is related to the beam angle, aircraft inertial approach speed U_0, and ship speed U_s, in the manner shown. The nominal values ($\bar{h}_R$, $\bar{V}_I$, $\bar{X}_{TD}$) are seldom obtained in practice because of motions of the ramp and intended touchdown point, air-wake-induced flight path deviations, and flight path deviations because of the pilot/aircraft system responses to FLOLS beam motions. It is important to note that the distributions illustrated in Fig. 4, for convenience, reference to a steady deck; in the actual analysis they are determined with reference to a moving deck and are composed of both aircraft perturbations and deck motions. As noted in Ref. 3, the correct method for combining the two can become an involved process, especially in those instances when motions of aircraft and deck are not independent.

Computing terminal landing errors involves combining air wake and ship motion inputs with the dynamics of the FLOLS and pilot/aircraft system and, simultaneously, mating the resultant aircraft terminal flight path parameters with the deck's kinematics as indicated by the terminal error equations in Fig. 1. This portion of the carrier landing analysis is straightforward except when confronted with interdependency of system elements and/or inputs (for example, when the FLOLS beam motions and, consequently, the aircraft perturbations are related to the deck motion).‡ Various computational methods have been utilized to contend with the multiple inputs, complex transfer functions, and time-varying nature of certain FLOLS stabilization configurations. These methods are noted in Ref. 1 and are described in detail in Ref. 3. Such complexity in the model is circumvented when using terminal error measurements directly; a piloted simulation system can be employed to obtain these measures, as illustrated subsequently.

‡ Reference 3 describes the application of the adjoint method for contending with this interdependency. Complexity also arises in an exact evaluation of that portion of the air wake which is correlated with ship motions. Fortunately, in this instance, the ship-motion-induced turbulence proved to have negligible effect on aircraft flight path, thereby permitting considerable simplification in the model description.

Landing Performance Metric

The dispersions obtained from the terminal landing error analysis leave much to be desired in assessing system performance. More confident judgments are possible if these distributions are transformed to operational performance indices. Probabilities of potential ramp strike, gear failure, and bolter are obtainable by suitably combining the dispersions with the basic arrestment geometry. The mechanics of this computation are illustrated in Fig. 5. Previously described Δh_R and ΔV_I distribution functions are replotted here, and the Δh_{TD} distribution is converted to an equivalent fore/aft dispersion of the hook touchdown point by the basic angle function $1/\beta_0$. Available safety margins are computed as the difference in maximum permissible and nominal operating values of these functions. The determination of margin exceedance probabilities is a standard computation routine applicable to Gaussian or normal distribution functions; the assumed normality in the present instance is generally supported by actual distribution measurements, such as those in Ref. 12, and the analysis in Ref. 13.

Without LSO waveoff action, the probability of a successful pass is $(1 - P_{h_R})(1 - P_{V_I})(1 - P_{X_{TD}})$; its reciprocal gives the minimum number of passes required for a successful landing. Conversely, P_{h_R}, P_{V_I}, and $P_{X_{TD}}$ separately represent the mutually exclusive probabilities of ramp strike, gear failure, and bolter which would result if waveoffs did not occur.

The LSO's actions significantly influence the actual performance measures; hence, the complete landing system performance matrix, shown in Fig. 6, includes the statistical LSO model. The term matrix refers to the derivation and interrelationships of a multiplicity of performance indices that are essential in evaluating carrier landing systems, namely, as

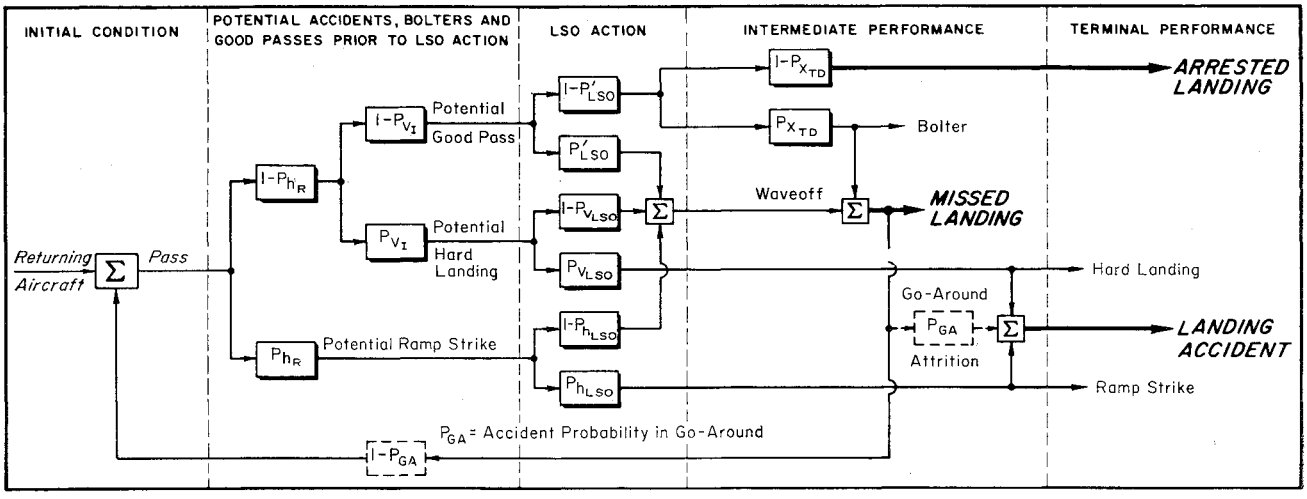

PERFORMANCE INDEX		SYMBOL	EQUATION
ARRESTED LANDING RATE	Per Pass	$P_{L/P}$	$(1-P_{X_{TD}})(1-P'_{LSO})(1-P_{V_I})(1-P_{h_R})$
BOLTER RATE	Per Pass	$P_{B/P}$	$P_{X_{TD}}(1-P'_{LSO})(1-P_{V_I})(1-P_{h_R})$
	Per Landing	$P_{B/L}$	$P_{X_{TD}}[1-P_{X_{TD}}]^{-1}$
WAVEOFF RATE	Per Pass	$P_{WO/P}$	$P'_{LSO}(1-P_{V_I})(1-P_{h_R})+(1-P_{V_{LSO}})(1-P_{h_R})P_{V_I}+(1-P_{h_{LSO}})P_{h_R}$
	Per Landing	$P_{WO/L}$	$[P'_{LSO}(P_{V_I})(1-P_{h_R})+(1-P_{V_{LSO}})(1-P_{h_R})P_{V_I}+(1-P_{h_{LSO}})P_{h_R}](P_{L/P})^{-1}$
MISSED LANDING RATE	Per Pass	$P_{ML/P}$	$P_{WO/P}+P_{B/P}$
	Per Landing	$P_{ML/L}$	$[P_{WO/P}+P_{B/P}](P_{L/P})^{-1}$
RAMP-STRIKE RATE	Per Pass	$P_{RS/P}$	$P_{h_{LSO}}P_{h_R}$
	Per Landing	$P_{RS/L}$	$[P_{h_{LSO}}P_{h_R}](P_{L/P})^{-1}$
HARD-LANDING RATE	Per Pass	$P_{HL/P}$	$P_{V_{LSO}}P_{V_I}(1-P_{h_R})$
	Per Landing	$P_{HL/L}$	$[P_{V_{LSO}}P_{V_I}(1-P_{h_R})](P_{L/P})^{-1}$
LANDING ACCIDENT RATE	Per Pass	$P_{A/P}$	$P_{h_{LSO}}P_{h_R}+P_{V_{LSO}}P_{V_I}(1-P_{h_R})$
	Per Landing	$P_{A/L}$	$[P_{h_{LSO}}P_{h_R}+P_{V_{LSO}}P_{V_I}(1-P_{h_R})](P_{L/P})^{-1}$

Fig. 6 Landing system performance matrix.

follows: 1) arrested landing rate $P_{L/P}$ and its inverse, the number of passes required for an arrested landing; 2) missed-landing rate P_{ML}; and 3) landing accident rate P_A. The matrix starts off on the left with the initial "aircraft-to-be-recovered" condition; a pass may be in process, either as an initial landing attempt or as a subsequent attempt following a waveoff or bolter. It ends on the right with one of only two possible terminal conditions, either "arrested landing" or "landing accident." The intervening aspects derive from previously discussed considerations. Note, however, that an additional element has been introduced, that is, the "go-around attrition" probability function P_{GA}, which is indicated by the two dashed boxes in the "missed-landing" feedback path. Although P_{GA} has not been employed in computations made to date, it is an important factor§ and has been inserted here to complete the picture. The equations relating the intermediate and terminal performance measures to the landing probabilities P_{hR}, P_{VI}, etc., and to the LSO action P_{LSO} and P_{LSO}', are listed in Fig. 6.

Compensated-Meatball Stabilization

The compensated-meatball stabilization concept is one of the more promising improvements derived from the landing system model analyses of Ref. 3. This FLOLS stabilization scheme involves commanding the pilot/aircraft system to follow deck motions by intentionally moving the FLOLS beam. When properly phase-advanced with respect to the deck motions, the FLOLS beam motions are intended to render aircraft responses synchronized with the vertical motion of the deck and thereby incur reduced terminal landing errors. The intentional moving of the beam is in direct conflict with the current FLOLS stabilization design philosophy, which aims at reducing beam motions as much as possible. This current philosophy is justifiably based on actual experience which shows that beam-chasing is dangerous in conjunction with presently employed FLOLS stabilization methods. It is therefore desirable to examine those factors behind the current design philosophy and see whether the CMS concept with its associated beam motions is a plausible method for stabilizing the FLOLS.

First, consider the interaction of the primary system elements, and in particular the two humans involved in the landing operation. Figure 7 provides a convenient guide for the cause/effect analysis which follows; specifically emphasized in the figure are the pilot's and LSO's views of the approach, and the significance of these views with respect to the overriding considerations—the terminal landing conditions. To be described are three different views of the approach, the effects on these views of current FLOLS stabilization methods, and the underlying philosophy of the CMS concept.

Three Different Views of the Landing Approach

1. *What the pilot sees*

The pilot's view of the approach in terms of height track is that furnished by the FLOLS, and involves only the inner-

§ The go-around attrition value is quite appreciable ($P_{GA} \doteq 0.5 \times 10^{-4}$) with respect to total carrier landing accidents ($P_{A/L} \doteq 3 \times 10^{-4}$)[2].

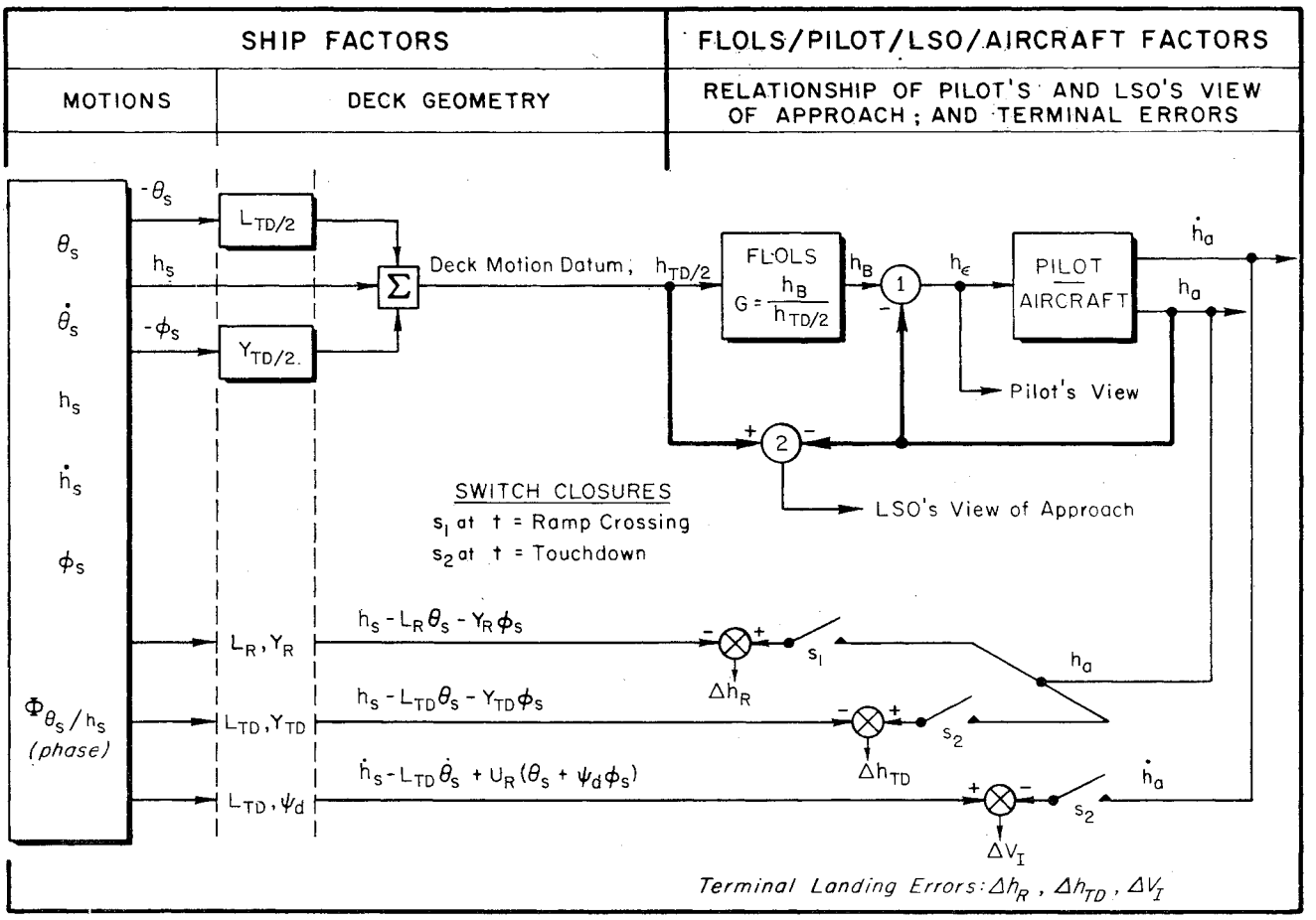

Fig. 7 Interaction between system elements.

most loop ① shown in Fig. 7. The height control piloting task in the approach is to maintain zero height track error ($h_\epsilon = 0$), i.e., keep the meatball image aligned with the datum bar. Since the FLOLS display is compensatory and provides error information only, the pilot cannot separate the beam motion components from the total error h_ϵ.¶ Consequently he must null out total errors, and he cannot easily and safely average out the motion of the beam as he is often told to do.

2. *What the LSO sees*

The LSO's view of the approach involves references other than FLOLS. Although these references are many, the cardinal reference for gaging terminal flight path during pitching deck conditions is the moving deck itself. Both the position of the ramp and the velocity of the deck are used as references by the LSO; these two can be conveniently combined into a singular deck motion datum $h_{TD/2}$,** as indicated.

The point of importance is that what the LSO sees is not the same as what the pilot sees because of the different visual references involved. Problematic situations arise because of these differing views, and these can be readily appreciated. For example, the pilot may be on a "roger-meatball" path ($h_\epsilon = 0$) all the way, while the LSO sees an oscillating, unstabilized-appearing path relative to his visual reference. The LSO's commands to the pilot may bear connotations of unrealism to the pilot, who in fact has a centered meatball.

3. *Terminal performance view of the approach*

What really counts are the terminal landing conditions, illustrated in Fig. 7 by the successive closure of switches S_1 and S_2, and whether a waveoff is given. When viewed in the context of optimum terminal performance, the LSO's view should prevail, i.e., the LSO's visual reference is more closely associated with terminal performance, as opposed to the pilot's continuous tracking visual reference. The pilot should, accordingly, subjugate his responses to the commands of the LSO; and when conflict arises the pilot should, somewhat unnaturally, disregard what he sees!

FLOLS Stabilization Interaction

Although current FLOLS stabilization methods attempt to remove all ship-motion-induced beam unsteadiness, some FLOLS beam motion exists for all current systems. For the line-stabilized FLOLS, for example, the beam translates in synchronism with ship's heave, i.e., $h_B = h_s$, and this beam motion generally leads the total deck vertical motion (representable by the illustrated deck motion datum) by about 0° to 90°,[3] depending on pitch/heave phasing and relative magnitudes. The closed-loop response of the pilot/aircraft system (loop ① in Fig. 7) can have appreciable lag with respect to beam motions— of the order of 180° or more, depending on ship motion frequencies. It is therefore conceivable that, although loop ① is by itself stable and properly closed by the pilot, loop ②, as viewed by the LSO, is nearly unstable! The

¶ Two possible exceptions need to be pointed out. First, the pilot can discern the h_B component from the visually sensed h_ϵ error on the basis of the expected dominant frequency of h_B. This argument is refuted later in the paper. The second possibility is that the pilot may "spot the deck," thereby derive additional information and use it by operating in a pursuit-like manner. Such behavior is acknowledged to exist, especially in daytime landings; however, it is dangerous and is emphatically discouraged.[14]

** The term $h_{TD/2}$ is the vertical motion with respect to inertial space of a point on the landing deck centerline, halfway between the ramp and intended touchdown point.

Table 1 Comparison of carrier landing accident rates, simulator/analytical results vs actual operations

Aircraft model	Accident rates per 10,000 landings: Simulator/model	Actual[a]
F-4	21.2	8.0
F-6	21.4	9.61
F-8	22.6	7.22
A-4	1.27	2.37

[a] Day/night average carrier landing accident rates based on NASC FY1954—1964 records; average calm sea-state conditions; mostly day landings.

degree of such impending instability is dependent on the magnitude and nature of ship motions; this is not a very consistent or safe-appearing view seen by the LSO. The current FLOLS stabilization design philosophy, i.e., attempting to provide $h_B = 0$, has two possible saving graces: it makes the piloting task easier and, more important, it eliminates the LSO's uncertainty as to what the FLOLS is telling the pilot. But what about the LSO's view, with respect to his reference, of a roger-meatball approach and, more important, what about the terminal landing errors?

Underlying Philosophy of CMS

The uppermost objective of the CMS scheme is to reduce terminal landing errors. Second, it attempts, where feasible, to make the pilot's view of the approach consonant with that of the LSO. The concept can be appreciated by the following line of reasoning: 1) working backwards, terminal landing errors are minimized by equating the h_a and $\dot{h}_a$ aircraft responses to the corresponding deck position and velocity parameters shown in Fig. 7; 2) a deck motion datum, shown as $h_{TD/2}$, is selected to represent the best-compromise aircraft response which will simultaneously minimize the Δh_R and ΔV_I terminal errors, i.e., those errors existing when switches S_1 and S_2 close; and 3) a specific stabilization form, G_c, for the FLOLS element is chosen to insure stability of loop ② in Fig. 7 and to achieve nearly synchronized aircraft/deck-motion-datum responses, i.e., $h_a/h_{TD/2} \doteq 1.0 \measuredangle 0°$. Thus, for a fast-responding pilot/aircraft system, the proper FLOLS stabilization logic would be $h_B/h_{TD/2} \doteq 1.0 \measuredangle 0°$, and resulting pilot and LSO views of the approach would be identical. For a more sluggish pilot/aircraft inner loop, the desired nearly synchronized responses are achieved by a FLOLS compensation form that cancels the amplitude distortion and phase lags of the pilot/vehicle system. Exact cancellation is obtained with a compensation filter G_c, configured with the inverse pilot/aircraft dynamic characteristics. The combined dynamics of the pilot, Y_p, and aircraft, Y_a, are expressed as

$$h_a/h_{TD/2} = Y_pY_a/(1 + Y_pY_a) \tag{1}$$

The corresponding desired compensation filter is therefore

$$G_c = (1 + Y_pY_a)/Y_pY_a \tag{2}$$

Equation (2) can be approximated with the closed-loop phugoid mode, $(\omega_p, \zeta_p)_{CL}$, which is dominant for height-following, i.e.,

$$G_c = K_c[(s^2/\omega_c^2) + (2\zeta_c s/\omega_c) + 1] \tag{3}$$

where $\omega_c \doteq (\omega_p)_{CL}$ and $\zeta_c \doteq (\zeta_p)_{CL}$.

The closed-loop phugoid parameters, $(\omega_p, \zeta_p)_{CL}$, differ from airplane to airplane. They range in value as follows:

$$\begin{array}{lccc} (\omega_p)_{CL} & 0.5 & \text{to} & 1.0 \text{ rad/sec} \\ (\zeta_p)_{CL} & 0.1 & \text{to} & 0.4 \end{array} \tag{4}$$

Ideally, the compensation parameters ω_c and ζ_c should be matched as closely as possible to the individual $(\omega_p)_{CL}$ and $(\zeta_p)_{CL}$ values. From an operational point of view, one fixed set of ω_c, ζ_c values would be preferable, representing the average expected values of $(\omega_p)_{CL}$ and $(\zeta_p)_{CL}$.

Simulation and Analysis

A night carrier landing simulation with severe deck motions was used by pilots to evaluate several FLOLS stabilization configurations. The simulator setup and experimental procedure are described in Ref. 1. Measurements and data analyses were performed in the following manner. 1) The performance measures taken for each pass were the terminal landing errors in ramp height, Δh_R; height over intended touchdown point, Δh_{TD} (equivalent to touchdown point error); and impact velocity, ΔV_I. 2) The error measurements for individual pilots were combined for specific aircraft/FLOLS-stabilization/ship-motion-frequency combinations, and means and standard deviations were computed. 3) The resulting error distribution functions were combined with the landing geometry to obtain the mutually exclusive probabilities P_{hR}, P_{VI}, and P_{XTD}, using the process illustrated in Fig. 5. 4) Missed-landing and accident rates, $P_{ML/L}$ and $P_{A/L}$, were determined using the "ninety-by-ten" LSO action model in conjunction with the performance matrix equations given in Fig. 6.

Comparison with Actual Carrier Landing Performance

Baseline data using the conventional line-stabilized FLOLS were obtained for four aircraft. Accident rates computed from the performance matrix are compared in Table 1 with actual landing accident rates experienced by those same four aircraft over a recorded 10-yr period. Considering the differences in simulated vs real carrier landing environments,†† the accident rates resulting from the simulator/model compare quite well with the actual data for all aircraft, with the possible exception of the A-4. The A-4 simulator accident rate, while lower than actually experienced, is nevertheless ranked correctly with respect to the other aircraft.

Comparison of Line-Stabilized and Fixed-Parameter-CMS FLOLS

The results of this evaluation are presented in Table 2 together with those pertinent landing geometry and LSO-action values used in the assessments. The fixed-parameter-CMS values employed in the tests [see Eq. (3)] were: $K_c = 1.0$, $\omega_c = 0.75$ rad/sec, and $\zeta_c = 0.3$. As discussed later, these were optimum for the F-6 aircraft.

The relative advantages of the two FLOLS stabilization methods can be more accurately assessed if a comparison is made of the best landing performance achievable with each system. Consider, for example, the F-4 results in the top half of Table 2 for a fixed $\beta_0 = 4°$. The F-4 accident rate of 21.2×10^{-4} with the line-stabilized FLOLS is composed almost exclusively of hard landings, with Ref. 1 showing that a large difference existed between P_{hR} and P_{VI}. This indicates that the pilot obtained better performance in clearing the ramp than in minimizing the impact velocity.‡‡ In this situation it would be desirable to reduce the basic angle in order to minimize the over-all probability of a landing accident. With the compensated-meatball-stabilized FLOLS, P_{hR} and P_{VI} are approximately equal,[1] and the 4° basic angle is almost optimum for minimizing over-all combined ramp strike and

†† Nighttime landing in a Sea State 6 was simulated, whereas daytime landing in a Sea State 0–1 more typically represents average actual conditions. Note also that the nighttime carrier landing accident rate is approximately three times that for daytime landings.

‡‡ The probability of a ramp strike is determined from the average ramp clearance, $\bar{X}_{TD} \tan\beta_0 + \overline{\Delta h_R}$, and the rms distribution of height errors at the ramp, $\sigma(\Delta h_R)$. Thus both the average flight path and the flight path dispersion influence ramp clearance performance.

Table 2 Landing performance summary for various aircraft, line-stabilized and fixed-parameter-CMS FLOLS

$(V_I)_{ultimate}$ = 24 ft/sec Wind-over-deck = 50 ft/sec $\bar{X}_{touchdown}$ = 234 ft $X_{last\ wire}$ = 294 ft			FLOLS basic angle β_0	FLOLS stabilization method	Probable accident and missed-landing rates per landing with LSO action, $P_{h_{LSO}} = P_{V_{LSO}} = P'_{LSO} = 0.1$ (see Fig.6)			
	Airc.	Airsp.			$P_{A/L}$	$P_{ML/L}$	Ratio of $(P_{A/L})_{CMS/LS}$	Ratio of $(P_{ML/L})_{CMS/LS}$
Fixed β_0	F-4	136 kt	4°	LS	0.00212	0.975		
				CMS	0.000402	0.470	0.19	0.48
	F-6	143 kt		LS	0.00214	0.865		
				CMS	0.000368	0.294	0.17	0.34
	F-8	141 kt		LS	0.00226	0.332		
				CMS	0.00347	0.252	1.5	0.76
	A-4	133 kt		LS	0.000127	0.429		
				CMS	0.000190	0.336	1.5	0.78
Idealized β_0	F-4	136 kt	2.51° 4.00°	LS	0.000424	1.52		
				CMS	0.000402	0.468	0.95	0.31
	F-6	143 kt	3.17° 2.71°	LS	0.000842	1.096		
				CMS	0.0000219	0.490	0.026	0.45
	F-8	141 kt	3.50° 2.92°	LS	0.00162	0.363		
				CMS	0.00142	0.297	0.88	0.82
	A-4	133 kt	3.62° 3.30°	LS	0.0000924	0.473		
				CMS	0.0000581	0.425	0.63	0.90

hard-landing accidents. The effects of a nonoptimum nominal glide path and piloting technique biases, e.g., "holding a high meatball," can be reduced by comparing landing performance indices determined for ideal basic angle operation. A convenient approximation to the ideal basic angle is that β_0 value yielding $P_{hR} = P_{VI}$. This basic angle can be readily determined from the relationships in Figs. 4 and 5, and is expressed as

$$\beta_0]_{\text{ideal}} = \frac{[(V_I)_{\text{ultimate}} - \overline{\Delta V_I}]\sigma(\Delta h_R) - \overline{\Delta h_R}\sigma(\Delta V_I)}{\bar{X}_{TD}\sigma(\Delta V_I) - (U_0 - U_s)\sigma(\Delta h_R)} \quad (5)$$

The implications of Eq. (5) are much more than those simply used here. More important, the equation states the logic by which β_0 might be continuously idealized as a function of known landing system variables and environment; that is, specific knowledge of $(V_I)_{\text{ultimate}}$ and U_0 values for individual aircraft, U_s, etc., as might be obtained from continuous on-line measurements and computations, may be advantageously utilized for continuous idealization of β_0.

The idealized FLOLS basic angles for each aircraft/FLOLS-stabilization combination and the corresponding landing performance indices are shown in the bottom half of Table 2. For the line-stabilized FLOLS, a value of $\beta_0 \doteq 3.5°$ is indicated by the simulation to be ideal for two of the four aircraft tested. In actual fleet operations, basic angles of 3.5° and 4° are used, depending on carrier size, operating environment, and many other operational considerations. Thus, the simulator results and the ideal basic angle concept are consistent with established operational carrier landing practice.

From the results in Table 2, the following tentative generalized conclusions are made:

1) Compensated-meatball stabilization can provide a good payoff, in terms of both reduced accidents and reduced missed-landings, when the compensation parameters are optimized for a particular aircraft. (The particular set of CMS parameter values used in the experiment matched closest to closed-loop pilot/aircraft phugoid values of the F-6 aircraft, and, correspondingly, the greatest improvement in landing performance was demonstrated for the F-6.)

2) A fixed-parameter compensation filter will definitely improve the landing performance for certain aircraft types, and for remaining aircraft types will provide a performance level at least equivalent to that derivable from the line-stabilized FLOLS.

3) The results suggest a variable-parameter compensation filter with which to separately optimize the landing performance of each aircraft type. Such a system would entail an operational procedure similar to the present one of setting specific static FLOLS roll angles to accommodate variations in individual aircraft hook-to-eye distances.

Variable-Parameter CMS and the Effects of the Aircraft Parameter $1/T_{\theta_2}$

The simulated CMS/FLOLS logic permitted simple alteration of the $h_B/h_{TD/2}$ amplitude/phase vs frequency characteristics. The flexibility was utilized in determining apparent optimum CMS parameter values to see whether similar payoffs are obtainable for aircraft other than the F-6. The resulting optimum CMS parameter values for each of the four aircraft considered are given in Table 3. The A-4 optimum values appear close to those found optimum for the F-6; slightly more lead at lower frequencies is needed for the A-4, and is obtainable by shifting the break frequency of the

Table 3 Optimum CMS parameters and aircraft $1/T_{\theta_2}$ values

Aircraft model	Optimum CMS parameters [see Eq. (3)] determined from simulator tests	$1/T_{\theta_2}$ (sec^{-1})
F-6	$\omega_c = 0.75$ rad/sec, $\zeta_c = 0.3$	0.690
A-4	$\omega_c \doteq 0.65$ rad/sec, $\zeta_c = 0.3$	0.630
F-4	$\omega_c < 0.5$ rad/sec	0.344
F-8	$\omega_c < 0.5$ rad/sec	0.476

compensation down from $\omega_c = 0.75$ to about 0.65 rad/sec. With the latter compensation values, the performance improvement for the A-4 is expected to be approximately the same as that previously described for the F-6 aircraft.

Such a happy state of affairs was not the case for either the F-4 or F-8 aircraft. Upon examination of the continuous tracking data for these two aircraft models, it was learned that the pilot/aircraft combinations involved could not develop the required crossover frequency values, which, for effective compensation, must be greater than the dominant ship motion frequencies. In effect, this means that if the pilot attempts to follow beam motions with elevator control, i.e., tries to hold a precisely centered meatball by biasing the attitude reference, he ends up with an unstable-appearing altitude loop. An intense effort by the pilot to reduce meatball errors results in a very poorly damped height control loop (loop ① in Fig. 7) which amplifies beam motions and causes large flight path overshoots; these are so large, in fact, that the aircraft tends to stray beyond the ±0.75° FLOLS beam envelope limits. Clearly, tight height control is not the technique to use with either the F-4 or F-8. Even a novice pilot will, after only two or three unsuccessful landing attempts, regress§§ to a low gain operation in the height loop; and only then will he have a marginal chance for a safe arrestment.

The pilot/aircraft closed-loop control problems with the F-4 and F-8 are directly traceable to the airframe parameter $1/T_{\theta_2}$.¶¶ Both the F-6 and A-4 aircraft are characterized by moderately large $1/T_{\theta_2}$ values. Table 3 shows that the experimentally determined optimum compensation break frequencies are close to the respective values of $1/T_{\theta_2}$, i.e., the experiments infer $(\omega_c)_{\text{optimum}} \doteq 1/T_{\theta_2}$.

A large value of $1/T_{\theta_2}$ permits a large bandwidth with reasonable damping in the altitude loop (loop ① in Fig. 7), and good height tracking performance is obtainable; conversely, small values of $1/T_{\theta_2}$ result in maximum bandwidths which are less than the dominant ship frequency and, consequently, poor altitude tracking occurs. The significance of the relative magnitude of the height loop crossover frequency to the ship motion frequency is more readily understandable by examining the results of a peripheral experiment, one specifically aimed at verifying the importance of $1/T_{\theta_2}$ in carrier landings. The A-4 aircraft dynamics were used in continuous tracking at a synthetically held fixed range from the ship with the pilot subject trying to hold a centered meatball. The stability derivative Z_w was systematically changed and the tracking records were analyzed to deduce the relationship of closed-loop pilot/aircraft height response to FLOLS beam motion input. Perfect beam-following corresponds to $h_a/h_B = 1.0 \angle 0°$, and occurred with $1/T_{\theta_2} \doteq 1.0$. As Z_w, and hence $1/T_{\theta_2}$, was lowered, the aircraft/beam-motion amplitude ratio and phase lag increased, becoming approximately $2.5 \angle -60°$ for $1/T_{\theta_2} \doteq 0.5$.*

§§ Reference 4 presents experimental human response data which show that crossover frequency or loop gain regression occurs, and explains the phenomenon in detail.

¶¶ $1/T_{\theta_2}$ is the larger of the two zeros in the aircraft's pitch-attitude-to-elevator transfer function, $\theta(s)/\delta_e(s)$, and is related to nondimensional aerodynamic terms by the approximate expression

$$1/T_{\theta_2} \doteq -Z_w = [\rho(U_0 + W)S/2m](C_{L_\alpha} + C_D)$$

where

S = wing area, ft²
m = aircraft mass, slugs
ρ = mass density of air, slugs/ft³
U_0 = aircraft inertia speed, fps
W = natural wind speed, fps
C_{L_α} = aircraft lift-curve slope, per rad
C_D = aircraft drag coefficient

* Phase lag can be decreased for the dominant second-order closed-loop mode by lowering the closed-loop damping ratio, but a larger maximum amplitude ratio occurs. Amplitude ratio and damping ratio are related by the approximate expression $AR_{\max_{db}} = -20 \log 2\zeta$.

At $1/T_{\theta_2} \doteq 0.4$ a bimodal pilot tracking technique was observed. The pilot felt he was operating near the maximum altitude loop gain possible without going entirely unstable, and the corresponding aircraft/beam-motion characteristics were determined to be $h_a/h_B \doteq 3.0 \angle -50°$. The pilot elected to regress to lower loop gain values and reduced his control responses to observed altitude errors. When this occurred, the phase lag between aircraft height response and beam motion input immediately increased to −180° and the corresponding amplitude ratio decreased to 0.5, i.e., $h_a/h_B \doteq 0.5 \angle -180°$. The effects of this piloting technique change are as follows. Note that an amplitude ratio of $|h_a/h_B| = 3.0$ signifies that the aircraft responds with height perturbations which are three times larger than the height traversed by the FLOLS beam at any given range from the ship. For the line-stabilized FLOLS at all ranges, the beam motion is equal in magnitude to the ship's heave motion. Thus, the reduction in closed-loop-altitude-response/beam-motion amplitude ratio from 3.0 to 0.5 is beneficial in terms of reduced meatball tracking errors and reduced landing errors due to ship motion. But, the required reduction in altitude loop gain has an adverse effect on the aircraft's height motions and the resulting landing errors due to the air wake disturbance (see Fig. 3).

Support for the Contended Importance of $1/T_{\theta_2}$

Both the simulation and analytical results indicate that $1/T_{\theta_2}$ has a significant influence on longitudinal control and, consequently, should be a primary factor in carrier landing terminal performance. Two questions that logically arise in this regard are: 1) Do actual operational accident data for individual aircraft show a dependency on the value of $1/T_{\theta_2}$? 2) Does an aircraft's $1/T_{\theta_2}$ value strongly influence the functional operation of the SPN-10 system in fully automatic carrier landings? Both questions are treated in the following discussion.

1. Inferred bivariate dependency of carrier landing accident rate on $1/T_{\theta_2}$ and approach speed

Figure 8 shows the relationship of total accident rate with $1/T_{\theta_2}$ and mean operational approach speed for the four aircraft previously discussed and for the A-3 and F-11. The values of operational accident rates, approach speeds, and $1/T_{\theta_2}$ were derived from the best sources available. These sources are enumerated in Ref. 1. The reason that approach speed is shown as a possible accident causative factor is that the landing system model predicts such a dependency (illustrated by the dashed curve in Fig. 8). By further postulating that $1/T_{\theta_2}$ is a significant factor, it is possible to explain some of the more notable apparent discrepancies between the predicted and actual accident rate vs approach speed relationships. It should be pointed out, however, that $1/T_{\theta_2}$ and approach speed are not independent parameters† and that high wing loading, low lift-curve slope airplanes (with consequent small $1/T_{\theta_2}$ values) tend to have higher approach speeds from other considerations.

The difference in accident rates for the A-3 and A-4 aircraft, which have approximately the same approach speed, appears to be explainable by their dissimilar $1/T_{\theta_2}$ values. Also, the data in Fig. 8 indicate that the F-4's accident rate, higher than expected on the sole basis of approach speed, may be significantly influenced by the small magnitude of its $1/T_{\theta_2}$ value. The F-6 has the highest accident rate of all the air-

† At first glance, the approximate expression for $1/T_{\theta_2}$ would appear to indicate that $1/T_{\theta_2}$ increases proportionally with approach speed. However, this is not necessarily true. For one thing, the drag coefficient decreases with increased approach speed. Second, the expression shown is a first-order approximation only, and other stability and control derivatives have an effect on the actual $1/T_{\theta_2}$ value.

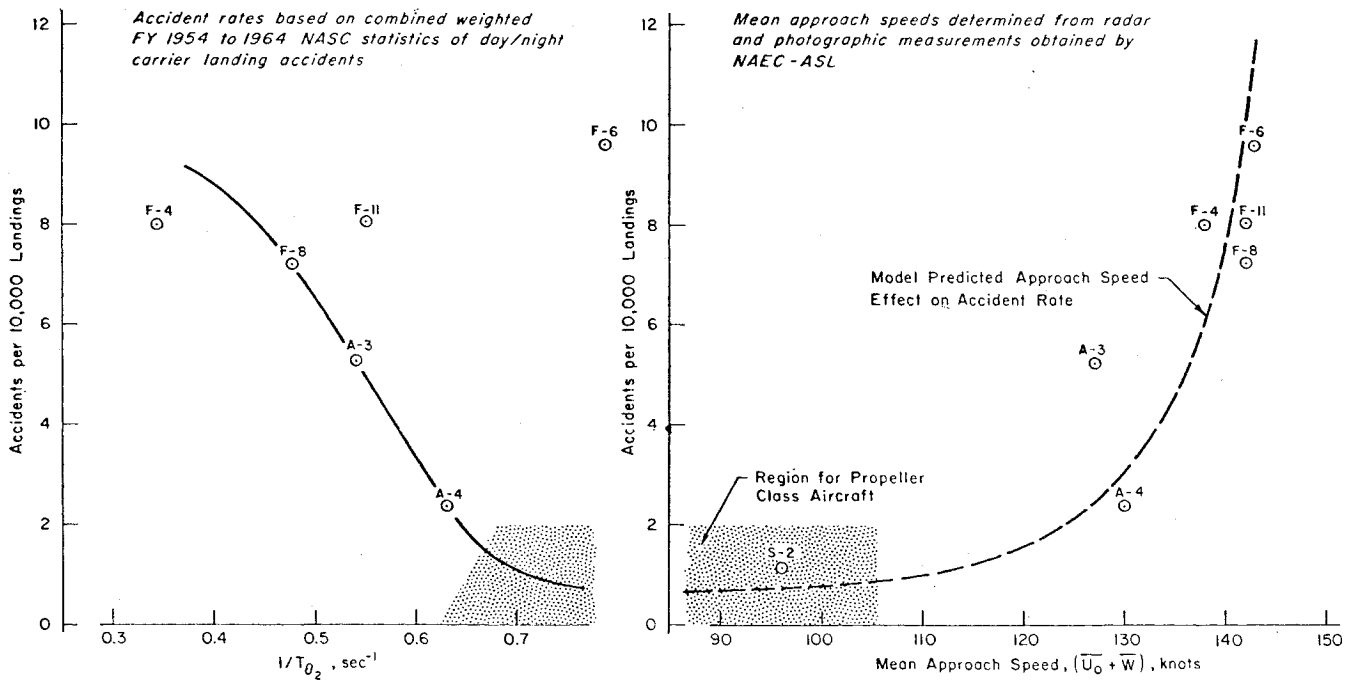

Fig. 8 Implied bivariate dependency of accident rate on $1/T_{\theta 2}$ and approach speed.

craft, and the considerations behind Fig. 8 would indicate that this is primarily because of its very high approach speed, since its $1/T_{\theta 2}$ value is quite large and hence "good." The separate effects of $1/T_{\theta 2}$ and approach speed do not explain the F-8's accident rate, especially with respect to that for the F-11.‡ With this one exception, the operational landing performance data strongly support the contended importance of $1/T_{\theta 2}$.

2. *Effect of $1/T_{\theta 2}$ on SPN-10 fully automatic carrier landing operation*

During automatic operation, the All-Weather Carrier Landing System controls the aircraft by transmitting data-link commands to a pitch-attitude-hold autopilot. The pitch attitude commands θ_c are related to the height error Z_e, which is the difference between a reference height and the radar-measured aircraft height. Position, rate, and integration terms are used to generate the command equalization, which is shown in general form in Eq. (6) (Ref. 15):

$$\frac{\theta_c}{Z_e} = K_{c0}K_c(X)\,\frac{1 + [\tau_r s/(s/10 + 1)] + 1/\tau_i s}{(s/5)^2 + s/5 + 1} \tag{6}$$

Equation (6) can be rewritten as

$$\frac{\theta_c}{Z_e} = K_{c0}K_c(X)\,\frac{\tau_i(\frac{1}{10} + \tau_r)s^2 + (\frac{1}{10} + \tau_i)s + 1}{\tau_i s(s/10 + 1)[(s/5)^2 + s/5 + 1]} \tag{7}$$

For a tightly closed pitch attitude autopilot loop, the aircraft's altitude response to θ_c has characteristic modes of the form

$$\Delta \doteq s(s + 1/T_{\theta 1})(s + 1/T_{\theta 2})[s^2 + 2(\zeta_{sp}\omega_{sp})_{CL}s + (\omega_{sp})_{CL}{}^2] \tag{8}$$

where the closed-loop short-period frequency, $(\omega_{sp})_{CL}$, is usually higher than that of the stick-fixed airplane and is higher than $1/T_{\theta 1}$§ and $1/T_{\theta 2}$. The main contributors to a lagging altitude response to pitch attitude commands are the $1/T_{\theta 1}$ and $1/T_{\theta 2}$ terms in Eq. (8); consequently, approximate cancellation of these terms is necessary to obtain good height response characteristics. Thus, the optimum SPN-10 equalization [Eq. (7)] should be directly established from the relationship

$$[\tau_i(\tfrac{1}{10} + \tau_r)s^2 + (\tfrac{1}{10} + \tau_i)s + 1] = (T_{\theta 1}s + 1)(T_{\theta 2}s + 1) \tag{9}$$

Solving for the rate and integration parameters,

$$\begin{aligned} \tau_r &= [T_{\theta 1}T_{\theta 2}/(T_{\theta 1} + T_{\theta 2} - 0.1)] - 0.1 \\ \tau_i &= T_{\theta 1} + T_{\theta 2} - 0.1 \end{aligned} \tag{10}$$

Values of $1/T_{\theta 1}$, $1/T_{\theta 2}$, and the corresponding optimum τ_i and τ_r parameters for an F-8 aircraft at several approach speeds are given in Table 4. These results compare favorably with those presented in Ref. 16 for SPN-10 operation with an F-8 at an approach speed of 133 knots ($\tau_r = 2.0$ sec, $\tau_i = 20.0$ sec) and confirm the importance of $1/T_{\theta 2}$.

Since $1/T_{\theta 1} \ll 1/T_{\theta 2}$, the rate term in the SPN-10 command equalization [Eq. (6)] is established primarily by $1/T_{\theta 2}$; namely $\tau_r \doteq T_{\theta 2} - 0.1$. Thus, for small $1/T_{\theta 2}$ aircraft, more lead equalization is required and the higher frequency height errors are amplified as pitch attitude commands. In manual landings, the pilot cannot derive rate information from the FLOLS visual meatball error until he is quite close to the ramp and consequently cannot generate similar outer loop equalization.

Conclusions

The previous discussion has shown that a complex interaction exists between desirable FLOLS stabilization character-

Table 4 Analytically determined optimum SPN-10 equalization parameters for an F-8 aircraft

Approach speed (knots)	Aircraft parameters		Optimum SPN-10 equalization from Eq. (10)	
	$1/T_{\theta 1}$ (sec^{-1})	$1/T_{\theta 2}$ (sec^{-1})	τ_r (sec)	τ_i (sec)
124	0.001	0.48	2.08	1002.(
133	0.052	0.463	1.95	21.{
141	0.071	0.477	1.83	16.:

‡ Note that the data for the "F" aircraft series lie in the very steep portion of the predicted $P_{A/L}$ vs approach speed curve. Segregation of $1/T_{\theta 2}$ and approach speed effects is very difficult in this speed region.

§ $1/T_{\theta 1}$ is the smaller of the two zeros in the pitch-attitude-to-elevator transfer function.

istics and other system elements, notably ship motion behavior and aircraft response. Accordingly, it is advisable to summarize the primary factors of concern and establish, in generalized terms, the potential payoffs of the CMS concept. First, we will attempt a generalization of the basic problem, drawing on the specifics that are detailed in the preceding discussions. Then, we will pose plausible solutions to the basic problem. Finally, we will indicate the potential performance improvements with compensated-meatball stabilization.

Basic Problem

The fundamental limit preventing best derivable terminal landing performance involves the airframe parameter $1/T_{\theta_2}$. A small value of $1/T_{\theta_2}$ can have extremely adverse effects on landing performance from many different considerations, e.g., pilot's inability to compensate the FLOLS-indicated height errors, deck-motion-induced errors, air-wake-induced errors, and contradicting pilot and LSO views of the approach. Only few currently operational carrier-based aircraft types are performance-limited by small $1/T_{\theta_2}$ characteristics. For the large $1/T_{\theta_2}$ airplanes, the full landing performance potential is not being realized because of presently inadequate FLOLS stabilization methods. Use of CMS allows full advantage to be taken of the aircraft's capability to follow height commands. Although "large" and "small" values of $1/T_{\theta_2}$ are, in the foregoing context, conveniently referenced to the dominant ship's frequency ω_s, the absolute $1/T_{\theta_2}$ value is also important. That is, the pilot's ability to make small but precise height adjustments and other precognitive inputs near the ramp, and to contend with air wake effects throughout the landing approach is strongly affected by the airframe's $1/T_{\theta_2}$ value.

A CMS logic using $G_c = 1/(Y_pY_a)_{CL}$ theoretically eliminates deck-motion-caused landing errors, regardless of the $1/T_{\theta_2}$ value, i.e., this logic theoretically negates the effects of limited pilot/aircraft height-tracking bandwidths. When $1/T_{\theta_2} \gtrsim \omega_s$, only approximate compensation, $G_c \doteq 1/(Y_pY_a)_{CL}$, is needed to greatly reduce deck-motion-caused landing errors. For the condition $1/T_{\theta_2} < \omega_s$, the effects of variations in the closed-loop phugoid mode are critical. Exact compensation, $G_c \equiv 1/(Y_pY_a)_{CL}$, is required for the latter instance, and is unattainable for manual control.

The basic problem is concentrated in the fact that when $1/T_{\theta_2} < \omega_s$, there is no way of achieving a centered "roger-meatball" without using "excessive" attitude and angle of attack overshoots. The pilot will not operate in this fashion, and chances are he will consider any automatic system that does so unacceptable. That is, regardless of attempts made to improve the altitude control bandwidth, such schemes cannot get around the physical limitations inherent in elevator control of altitude with a low lift-curve slope and high wing loading airplane.

Basic Solutions

The obvious solution is to increase $1/T_{\theta_2}$ or eliminate its importance or decrease ω_s. For designs now on the drawing board increasing $1/T_{\theta_2}$ is a matter of properly selecting wing area, planform, sweep, and aspect ratio. Extensible flaps and slats can also help somewhat by effectively increasing the wing area for the landing configuration. For airplanes now flying there is no easy solution. Obviously the effective lift-curve slope could be augmented by feedbacks to the flap, but this strategem is probably more costly and less effective than direct lift control. Direct control of lift through a fast-operating flap drive and a suitable auxiliary control completely sidesteps the problems inherent in lift control through elevator action. Preliminary studies and flight test of such a system[17] have shown greatly improved altitude control for small $1/T_{\theta_2}$ aircraft.

Decreasing the effective ship motion frequency is a possibility that should not be overlooked. Ship motion frequency can be reduced directly by reducing ship's speed.[18] However, the resulting increased closing speed because of the reduced wind-over-deck or operational difficulties in achieving "standard" wind-over-deck at reduced ship speeds both offset the potential benefits derivable in this way.

Deck motion prediction can be used to reduce the effective ship motion frequency. For example, with perfect prediction the effective ship motion frequency is zero. Less perfect but perhaps more practical, the LSO's prediction of deck position and velocity could be used to advantage in conjunction with an inertially stabilized FLOLS beam. Here the LSO can advise the pilot to hold a high or low meatball with an effective command frequency well below that of the actual deck motion.

Indicated Performance Improvement Presently Derivable from CMS

Even without the previous "solutions," it appears that CMS can provide improved landing performance over that achieved with present FLOLS stabilization methods. The ideal CMS logic is one which produces compensated beam motions nearly synchronized with the deck motion datum for deck motion frequencies smaller than the aircraft's $1/T_{\theta_2}$ value and no beam motions at frequencies greater than $1/T_{\theta_2}$. The potential payoff for CMS is, consequently, a function of the particular aircraft's $1/T_{\theta_2}$ value with respect to the dominant ship motion frequency. The latter relationship provides a convenient index with which to assess expected gains, as follows.

$1/T_{\theta_2} < \omega_s$

A modest reduction in landing accident and missed-landing rates appears feasible. The pilot's and LSO's view of the approach become more nearly alike, and pilot workload is considerably reduced because high-frequency beam motions are essentially zero. The pilot must rely on the LSO's judgment concerning predicted deck position and velocity, and the LSO must take a more active part in controlling the landing.

$1/T_{\theta_2} \doteq \omega_s$

CMS should provide an impressive reduction in accident and missed-landing rates. The analytical/experimental results for Sea State 6 operation indicate a payoff relative to a line-stabilized system as follows: reduced landing accident rate by a factor of 10; reduced missed-landing rate by a factor of 2. Additionally, the pilot's and LSO's views of the approach are more nearly alike with CMS.

$1/T_{\theta_2} > \omega_s$

CMS theoretically eliminates deck-motion-caused landing errors, and provides identical pilot and LSO views of the approach.

References

[1] Durand, T. S. and Wasicko, R. J., "An analysis of carrier landing," AIAA paper 65-791 (November 1965).

[2] "U. S. Navy aircraft accident statistics, fiscal year 1964," U. S. Naval Aviation Safety Center, U. S. Naval Air Station, Norfolk, Va. (October 29, 1964).

[3] Durand, T. S. and Teper, G. L., "An analysis of terminal flight path control in carrier landings," Systems Technology Inc. TR-137-1 (August 1964).

[4] McRuer, D., Graham, D., Krendel, E., and Reisener, W., Jr., "Human pilot dynamics in compensatory systems—Theory, models, and experiments with controlled element and forcing function variations," Air Force Flight Dynamics Lab., AFFDL-TR-65-15 (January 1965).

[5] Durand, T. S., "Theory and simulation of piloted longitudinal

control in carrier approach," Systems Technology Inc. TR-130-1 (September 1963).

[6] Lehman, A. F., "An experimental study of the dynamics and steady-state flow disturbances encountered by aircraft during a carrier landing approach," Oceanics Inc. Rept. 64-16 (September 1964).

[7] Lehman, A. F. and Kaplan, P., "Experimental model studies of the dynamic velocity fluctuations existing in the air wake of an aircraft carrier," Oceanics Inc. Rept. 65-21, Pts. I and II (March 1965).

[8] Barnett, W. F. and White, H. E., "Comparison of the airflow characteristics of several aircraft carriers," David Taylor Model Basin Aero. Rept. 1008 (May 1963).

[9] "Optimum wind-over-deck for shipboard recovery operations with carrier based airplanes," Rept. 2, Final Report, Supplement to Naval Air Test Center Rept. RA1200001 (RSSH-31003) Ser. FT2222-215 (July 12, 1962).

[10] Waldron, S., "The effect of ship length, ship motions and landing geometry upon the safety of carrier operations," Office of the Chief of Naval Operations, Naval Warfare Analysis Group, Study 20 (October 16, 1961).

[11] "Review of fleet carrier landing doctrine; Report of," Naval Air Test Center Rept. 5213, FT2222-186 (October 5, 1962).

[12] Bowe, J. T. and Scheindlinger, S., "Statistical presentation of landing parameters for models A-3B, A-4C/E, F-4B, and RF-8A/F-8C aircraft aboard the USS MIDWAY (CVA-41) in the WESTPAC area," Naval Air Engineering Center Rept. NAEC-ASL-1074 (March 1, 1965).

[13] Hoy, W. W., "A method for establishing landing design criteria for carrier-based airplanes," Chance Vought Corp. Rept. 2-53400/2R367 (August 1962); also Chance Vought Corp. Rept. 2-53400/3R460 (June 1963).

[14] Netherland, R. M., "The total approach," U. S. Naval Aviation Safety Center, U. S. Naval Air Station, Norfolk, Va., Vol. 10, No. 9, pp. 1–22 (March 1965).

[15] Powell, F. D. and Theoclitus, T., "Study of an automatic carrier landing environment with the AN/SPN-10 landing control central," Bell Aerosystems Co. Rept. 6026-932001 (April 1, 1965).

[16] "Aircraft landing system compatibility study, F8U-2NE, AN/SPN-10," Bell Aerosystems Co. Rept. 60003-080 (November 1960).

[17] Etheridge, J. D. and Mattlage, C. E., "Direct lift control as a landing approach aid in the F-8C airplane, simulator and flight tests," Ling-Temco-Vought Inc. Rept. 2-53310/4R-175 (December 31, 1964).

[18] Kaplan, P. and Sargent, T. P., "Theoretical study of the motions of an aircraft carrier at sea," Oceanics Inc. Rept. 65-22 (January 1965).